BIBECHANA
ISSN 2091-0762 (Print), 2382-5340 (Online)
Journal homepage: http://nepjol.info/index.php/BIBECHANA
Publisher: Department of Physics, Mahendra Morang A.M. Campus, TU, Biratnagar, Nepal

Structural and Electronic Properties of Intercalated Transition Metal Dichalcogenides Compounds

Vandana B. Parmar*, Aditya M. Vora+
Department of Physics, University School of Sciences, Gujarat University, Navrangpura, Ahmedabad 380 009, Gujarat, India
Email: *vandanaparmar3996@gmail.com
+voraam@gmail.com

Article Information:
Received: December 31, 2021
Accepted: January 30, 2022

Keywords:
Density Functional Theory (DFT)
Generalized Gradient Approximation (GGA) Quantum ESPRESSO code
Intercalated compound

ABSTRACT
The structural and electronic properties of Transition Metal Dichalcogenides Compound (TMDC) TiS_2 and its intercalated compound like $FeTiS_2$ are reported in the present work using Density Functional Theory (DFT). The Generalized Gradient Approximation (GGA) with ultra-soft pseudopotential are used under Quantum ESPRESSO code. From the theoretical data, it is concluded that, the energy band structure of the TiS_2 material has been a small indirect band gap and possess a semiconductor characteristic, while the doped intercalated compound like $FeTiS_2$, the energy bands are overlapped in the Fermi region, which possess metallic characteristics. Also, $FeTiS_2$ is a ferromagnetic material with spin up and spin down nature observed from the band structure data.

DOI: https://doi.org/10.3126/bibechana.v19i1-2.46397

1. Introduction

Studies of Transition Metal Dichalcogenides Compound (TMDC) have shown considerable attention during last many years. Layered transition metal dichalcogenides (LTMCDs) have applications in various areas including lubrication, catalysis, photovoltaics, supercapacitors, and rechargeable battery systems [1]. Hence, the dimensionality of TMDC are also plays a significant role in their basic physical properties [1]. The study of structural and electronic properties of material gives a basic understanding of the materials [2]. Fang *et al.* [3] have reported ab-initio band-structure based calculations for bulk, single slab, and thin films of TiX_2 (X=S, Se) using the localized spherical wave method. The density functional theory (DFT) based formulation are found more useful for computing the structural and electronic properties of materials [4-11]. The guest 3d atom have transferred the charge from transition metal Fe-atom to the self-

intercalated compound like TiS_2 reported by Friend and Yoffe [12]. The generalized chemical formula for TMDCs is MX_2, where M represents the Transition metal of group IV, V and VI of the periodic table and X is the chalcogens element. Therefore, the TMDCs have shown more than 40 different combinations and have shown distinctive properties too.

Generally, in TiS_2, the layer of Ti atom is sandwiched between two Sulphur layers. Both atoms are attracted with very weak van der Wall's force and having a very small indirect bandgap between them. Because of this, the guest Fe atom can be easily intercalated into pure TiS_2 compound. Hence, the Fe-S bonds are much stronger than the Ti-S bonds in such $FeTiS_2$compound [13]. In both materials, the strong hybridization occurs in the 3d-states of Fe, 3d-states of Ti and 3p-states of S, respectively [14-19]. In electronic property calculation,the $FeTiS_2$ has a spin polarized fully relativistic band structure. In which, the energy bands of TiS_2 are not overlapped near the Fermi region while in the case of the$FeTiS_2$, they are overlapped near the Fermi region. According to this, the TiS_2 has a semiconductor nature while $FeTiS_2$ has a metallic nature.

2. Computational Methodology

All the calculations of structural and electronic properties are performed under DFT environment by using Quantum Espresso code [20] with Burai [21] in our computational laboratory. The structural optimization and the electronic properties such as band structure, density of states (DOS), partial density of states (PDOS) and total density of states (TDOS) of the aforementioned materials are reported using Generalized Gradient Approximation (GGA) [22] with Perdew–Burke–Ernzerhof (PBE) [23] and ultra-soft pseudopotential [24].

3. Results and Discussion

3.1 Structural optimization

Both the TiS_2 and $FeTiS_2$ compounds are having CdI_2-type layer structures. In which, the layer of Ti is sandwiched between two layers of Sulphur and the unit cell contains four atoms. In the unit cell the position of Ti is a 1a and those of two S atoms are in 2d (1/3, 1/3,0.2501) and (2/3,1/3,-0.2501), respectively. Therefore, the construction consists of S-Ti-S sandwich type structure, which is shown in Fig. 1. It is separated by in Z direction from the van der Wall's gap [18]. In a very weak van der Wall's attraction between the interlayers of Ti and S, the guest 3d atom like Fe can be easily intercalant in pure TiS_2. Therefore, the Fe atom having a lattice position is 1b (0, 0, 0.5) in the structure and formulate the hexagonal crystal structure with space group $P\bar{3}ml$ [164] as shown in Fig. 2. In $FeTiS_2$, the lattice parameters are a = 3.4395Å and c = 5.9303Å. The Brillouin zone (IBZ) for hexagonal crystal structure is shown in Fig. 3.

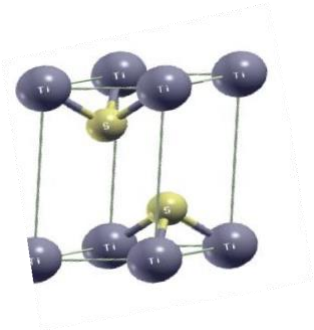

Fig. 1 – Crystal structure of TiS_2

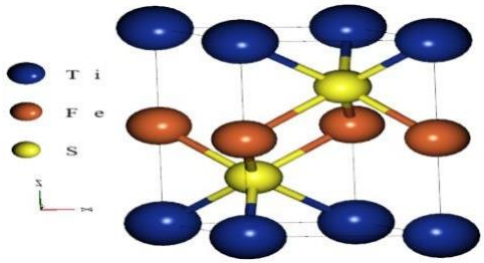

Fig. 2 – Crystal structure of $FeTiS_2$

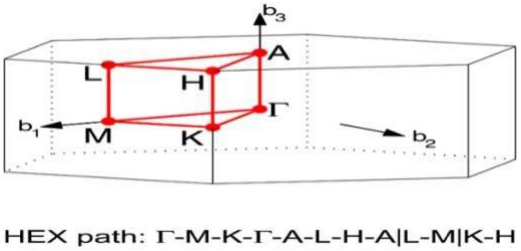

Fig. 3 – Brillouin zone for hexagonal structure

3.2 Electronic properties

In electronic properties, the energy band structure, density of states (DOS), total density of states (TDOS) and partial or projected density of states (PDOS) of the studied are reported.

3.3 Band structure

The energy band structures for TiS_2 material are plotted in Fig. 4 with the path of the **k**-points is taken on the high symmetry points. Such path is of the order of $\Gamma \rightarrow M \rightarrow K \rightarrow \Gamma \rightarrow A$. The energy band structures of TiS_2 are displayed in the energy range of -10.0 eV to 10.0 eV. The **k**-path of the band structure is highly symmetric directions with the irreducible Brillouin zone (IBZ). Generally, the energy band lines are not overlapped near at the Fermi region. Hence, the TiS_2 band structure has a semiconductor nature with small indirect bandgap [17].

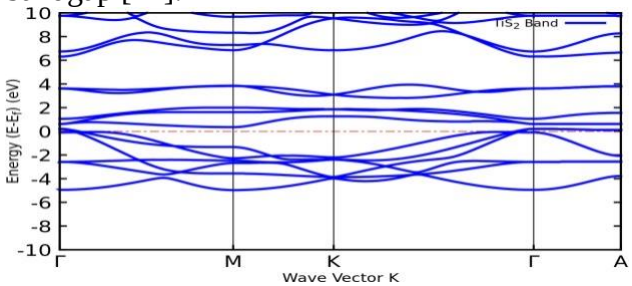

Fig. 4 – Electronic band structure of TiS_2

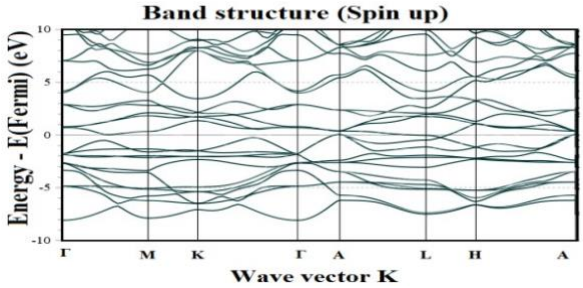

Fig. 5 – Electronic band structure of $FeTiS_2$ spin up

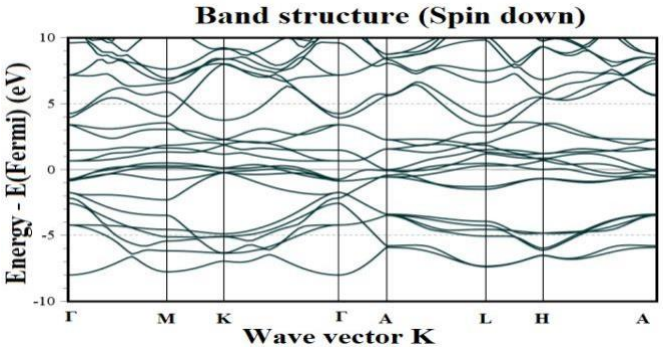

Fig. 6 – Electronic band structure of $FeTiS_2$ spin down

The energy band structures of $FeTiS_2$ material are shown in Figs. 5 and 6. Here, the energy band lines are overlapped near at the Fermi region. Therefore, the conduction band and valance band are crossed over to each other near at the Fermi region in the energy range of -5.0 eV to 5.0 eV. Hence, we conclude that the $FeTiS_2$ intercalated compound has a metallic characteristic whereas TiS_2 has a semiconductor characteristic. Also, according the spin up and spin down band structures of $FeTiS_2$, the ferromagnetic nature of the said compound are observed.

3.4 Density of States (DOS)

From the partial or projected DOS, the contributions from the individual orbitals like s, p, d and f of dissimilar materials are studied [25]. Here, we have applied the tetrahedral method for taking integration over the Brillouin zone to compute the DOS of the materials.

Figs. 7 and 8, show the TDOS and PDOS for TiS_2 compound. It is plotted in the energy range between -10.0 eV to 10.0 eV. In TDOS below the Fermi region, the electron density maximum at 9.0 states/eV at a point -3.0 eV. While, above the Fermi region, the electron density maximum at 7.0 states/eV at a point 2.0 eV, respectively. The DOS at the Fermi region is shown minimum. The 3d-states of Ti and 3p-states of S are drawn in the graph

of PDOS of TiS_2. Here, the 3d-states of Ti are mainly contributed to the conduction band, while 3p-states of S are mainly contributed to the valance band only, which can easily be observed from the figure of PDOS. Therefore, the TiS_2 shows a semiconductor nature.

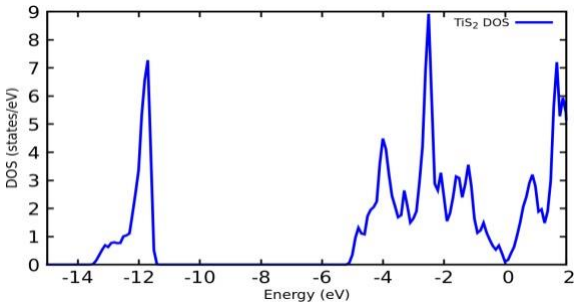

Fig. 7 – Total DOS of TiS_2

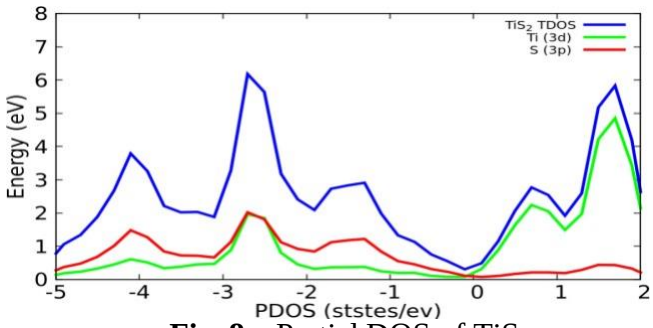

Fig. 8 – Partial DOS of TiS_2

The TDOS and PDOS of $FeTiS_2$ material are shown in Figs. 9 and 10. It is planned in the energy range between -10.0 eV to 10.0 eV in spin up and spin down energy states. In TDOS below the Fermi region, the electron density found maximum at 6.0 states/eV at a point -2.0 eV in spin up DOS and 3.5 states/eV at a point -4.5 eV in spin down DOS, respectively. While, above the Fermi region, the electron density maximum found at 2.0 states/eV at a point 3.5 eV in spin up and 4.5 states/eV at a point 2.5 eV in spin down DOS, respectively. The DOS at the Fermi region is shown at 2.5 states/eV. Similarly, in PDOS of $FeTiS_2$ the 3d-states of Fe and Ti are mainly paid to the conduction band, while 3p states of S are mostly contributed to the valance band only. Hence, the metallic nature of $FeTiS_2$ is easily seen.

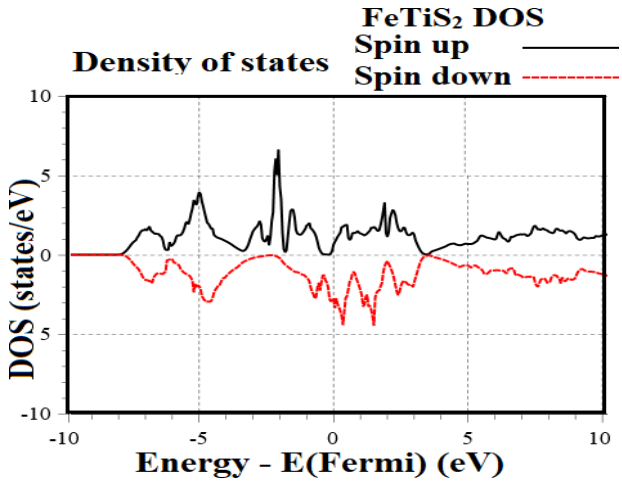

Fig. 9 – Total DOS of $FeTiS_2$

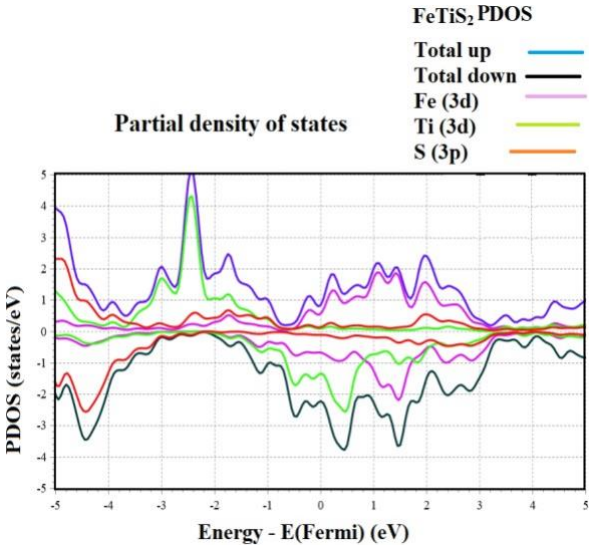

Fig. 10 – Partial DOS of $FeTiS_2$

Conclusion

Finally, we conclude that, the structural and electronic properties of intercalated TMDC compounds are successfully caried out using Quantum Espresso code with Burai software under DFT environment with GGA-PBE and ultrasoft pseudopotential. From the electronic band structure data, the semiconducting or semimetallic behaviour of TiS_2 and metallic nature of their interacted compound such as

$FeTiS_2$ are easily observed. Also, from the spin up and spin down electronic configuration, it is noted that the $FeTiS_2$ exhibits ferromagnetic nature.

Acknowledgment

We sincerely acknowledge the computational facility developed under DST-FIST programme from the Department of Science and Technology, Government of India, New Delhi, India and financial assistance under DRS-SAP-II from University Grants commission, New Delhi, India.

References

1. Z. Y. Zhu, Y. C. Cheng, and U. Schwingenschlögl, Phys. Rev. B84, 153402 (2011).
2. Q. H. Wang, K. K. Zadeh, A. Kis, J. N. Coleman and M. S. Strano, Nature Nanotech., 699(2012)712.
3. C. M. Fang, R. A. de Groot and C. Hass, Phys. Rev. B56 (1997)4455.
4. Vidit B. Zala, A. M. Vora and P. N. Gajjar, AIP Conf. Proc. 2100 (2019)020027.
5. H. S. Patel, V. A. Dabhi, A. M. Vora, in: D. Singh, S. Das, A. Materny (Eds.), Advances in spectroscopy-molecules to materials, Springer Proc. Phys. 236 (2019)389.
6. V. A. Dabhi, H. S. Patel, A. M. Vora, AIP Conf. Proc. 2224 (2020) 030003.
7. H. S. Patel, V. A. Dabhi and A. M. Vora, AIP Conf. Proc. 2224(2020)030006.
8. V. B. Parmar and A. M. Vora, East Eur. J. Phys. 1(2021)93.
9. V. B. Parmar and A. M. Vora, Eurasian J. Phys. Fun. Mater. 5(2021)116.
10. V. B. Parmar and A. M. Vora, KCG e-Journal of Sci. 30(2021)1.
11. V. B. Parmar and A. M. Vora, Armenian J. Phys.14(2021)37.
12. R. H. Friend and A. D. Yoffe, Adv. Phys., 36(1987) 1.
13. J. A. Wilson and A. D. Yoffe, Adv. Phys, 18(1969)193.
14. N. Suzuki, Y. Yamasaki and K. Motizuki, j De Physique. Solid State Phys. C, 8(1998)49201.
15. T. Yamasaki, N. Suzuki and K. Motizuki, J. Phys. C: Solid State Phys. 20(1987) 395.
16. T. Matssushita, S. Suga and A. Kimuta, Phys. Rev. B. 60(1999)1678.
17. Y. Ueda, H. Negishi, M. Koyana and M. Inoue, Solid State Comm. 57(1986)839.
18. Y-S. Kim, J. Li, I. Tanaka, Y. Koyama and H. Adachi, Mat. Trans. Jim, 8(2000)1088.
19. Y. Sharma, S. Shukla, S. Dwivedi and R. Sharma, Adv. Mater. Lett, 6(2015)294.
20. P. Giannozzi, S. Baroni, N. Bonini, M. Calandra, R. Car, C. Cavazzoni, D. Ceresoli, G.Chiarotti, M.Cococcioni, I. Dabo and A. Dal Corso, J. Phys. Condens. Matter**.** 21 (2009)395502.
21. http://nisihara.wixsite.com/burai
22. J. P. Perdew, J. Chevary, S. Vosko, K. Jackson, M. Perderson, D. Singh and C. Fiolhais, Phys. Rev. B48 (1993)4978.
23. J. P. Perdew, K. Burke and M. Ernzerhof, Phys. Rev. Lett. 77(1996)3865
24. http://www.quantum-espresso.org/pseudopotential.
25. Q. Bin, Z. Guo-Hua, LI Di, W. Jiang-Long, Q. Xiao-Ying, Z. Zhi, Chinese Phys. Lett. 24 (2007) 1050.